

THE TRIPLE LATTICE PETS

REN YI

ABSTRACT. Polytope exchange transformations (PETs) are higher dimensional generalizations of interval exchange transformations (IETs) which have been well-studied for more than 40 years. A general method of constructing PETs based on multigraphs was described by R. Schwartz in 2013. In this paper, we describe a one-parameter family of multigraph PETs called the triple lattice PETs.

We show that there exists a renormalization scheme of the triple lattice PETs in the interval $(0, 1)$. We analyze the limit set Λ_ϕ with respect to the parameter $\phi = \frac{-1+\sqrt{5}}{2}$. By renormalization, we show that Λ_ϕ is the limit of embedded polygons in \mathbb{R}^2 and its Hausdorff dimension satisfies the inequality $1 < \dim_H(\Lambda_\phi) = \log(\sqrt{2}-1)/\log(\phi) < 2$.

1. INTRODUCTION

Polytope exchange transformations (PETs) are dynamical systems that generalize interval exchange transformations (IETs). The definition of PETs is given as follows:

Definition 1.1. Let X be a polytope. A *polytope exchange transformation (PET)* is determined by two partitions of small polytopes $\mathcal{A} = \{A_i\}_{i=1}^m$ and $\mathcal{B} = \{B_i\}_{i=1}^m$ of X . For each $A_i \in \mathcal{A}$, there exists a vector V_i satisfying the property that

$$B_i = A_i + V_i.$$

A PET $f : X \rightarrow X$ is defined by the formula:

$$f(x) = x + V_i, \quad \forall x \in \text{Int}(A_i).$$

We call V_i a translation vector of f on A_i . Note that the PET f is not defined on the boundary ∂A_i for each i .

Now, we introduce a coding of system of PETs. Given an initial point $p \in X$, we associate its *coding* which is a sequence $\omega = \omega_0\omega_1 \cdots$ for $\omega_n \in \{1, \dots, m\}$ defined by

$$\omega_n = i \quad \text{if } f^n(p) \in A_i.$$

- Definition 1.2.**
- (1) A point is called *periodic* if $f^n(p) = p$ for $n \in \mathbb{Z}_+$.
 - (2) Suppose $p \in X$ is a periodic point of the map f . There exists a maximal subset Δ_p containing p such that the coding for each point in Δ_p is same as the one for p . We call the set Δ_p a *periodic tile* of p .
 - (3) The union of all periodic tiles in X is called the *periodic pattern* which is denoted by Δ .

2010 *Mathematics Subject Classification.* Primary 37E20; Secondary 37E05.

Key words and phrases. Polytope exchange transformations, symbolic dynamics.

However, it is unnecessary that every point in X is periodic. We are interested in the case when Δ is dense.

Definition 1.3. When Δ is dense, we define the *limit set*, denoted by Λ , as the set of points such that every neighborhood of the point in Λ intersects infinitely many periodic tiles.

Note that the limit set Λ contains all the points with well-defined and arbitrarily long orbits. We call such points *aperiodic points*. The union of all aperiodic points is called *aperiodic set* with notation Λ' .

1.1. Background. The one-dimensional example of PETs are interval exchange transformations (IETs) which have been studied extensively ([12], [18], [19] and [20]). One simple construction of of dimension two or higher PETs comes from the products of IETs. Haller generalize this construction by introducing *rectangle exchange transformations* [10]. Haller establishes criterions of minimality for rectangle exchange transformations.

The dynamical systems of *piecewise isometry* are closely related to PETs. Early examples of piecewise isometries are studied in the paper [1] and [6]. Let $T : X \rightarrow X$ be a piecewise isometry on a polytope X . If we restrict the isometry on each piece to either a translation or a rotation by $q\pi$ for $q \in \mathbb{Q}$, we call the map T a *piecewise rational rotation*. (See [2], [8], [14] and [13] for references.) There is a natural construction of PETs from piecewise rational rotations. Let $T : X \rightarrow X$ be a piecewise rational rotation. There exists a PET $\tilde{T} : \tilde{X} \rightarrow \tilde{X}$ in the covering space (\tilde{X}, π) of X so that $\pi \circ \tilde{T} = T \circ \pi$.

In [17], Schwartz introduce a general method of constructing PETs in all dimensions based on multigraphs (see Section 1.2). Let G be a multigraph such that each vertex is labeled by a convex polytope and each edge is labeled by a Euclidean lattice. Moreover, a vertex is incident to an edge if and only if the vertex label is a fundamental domain of the edge label. There is a functorial homomorphism between the fundamental group $\pi_1(G, x)$ for a base vertex $x \in G$ and the group $\text{PET}(X)$ of PETs defined on the labeled polytope X of x . We call the resulting systems *the multigraph PETs*. Schwartz provides a one-parameter family of PETs called *octagonal PETs* which corresponds to bigons (two vertices connected by two edges). He shows that there is a local equivalence between outer billiards on semi-regular octagons and octagonal PETs.

Few general results of PETs or piecewise isometries are known. Gutkin and Haydn [9] proved that piecewise isometries have zero topological entropy in dimension two. In the paper [4], Buzzi shows that the statement holds true in all dimensions. Our lack of understanding comes from the dynamics on the set whose orbits are not periodic. For example, we would like to understand the minimality or ergodicity on the set. More importantly, we would like to know if it is possible to construct a recurrent PET in dimension two or higher.

The scheme of renormalization is used to understand PETs (or more generally, piecewise isometries) in a lot of cases. Renormalization is a tool to zoom into the space and accelerate the orbits of points along time. To see this, we provide a basic definition:

Definition 1.4. Let Y be a subset of X . Given a map $f : X \rightarrow X$, the *first return* $f|_Y : Y \rightarrow Y$ is a map assigns every point $p \in Y$ to the first point in the forward

orbit of p lying in Y , i.e.

$$f|_Y(p) = f^n(p) \quad \text{where } n = \min\{f^k(p) \in Y\} \quad k > 0.$$

For IETs, Rauzy induction [15] provides a renormalization scheme. A classical example of renormalizable piecewise isometries is described in the survey paper [7] by Goetz. In the paper [13], Lowenstein develops a general theory of piecewise rational rotations. Hooper gives the first example of PETs in 2-dimensional parameter space which is invariant under renormalization [11]. The renormalization scheme arises from collapsing the reducing the loops in Truchet tilings. A recent paper [3] studies an example of piecewise isometries which is very similar to Hooper's example. A renormalization scheme of the system is discovered through a symbolic coding of the system. In [17], Schwartz shows that there is a renormalization scheme on the one-parameter family of octagonal PETs. Moreover, he finds that the hyperbolic triangular group $(2, 4, \infty)$ acts on the parameter space by linear fractional transformation as a renormalization symmetry group.

1.2. Multigraph PETs. Here we describe a construction of PETs in all dimensions called *multigraph PETs*, which is introduced by Schwartz in [16].

Definition 1.5. A *multigraph* is a monogon-free graph such that two vertices may be connected by more than one edge.

Let $G = (V, E)$ be a multigraph such that every vertex $v \in V$ is labeled by a convex polytope and every edge $e \in E$ is labeled by a Euclidean lattice. Moreover, two vertex v_0 and v_1 are connected by an edge e iff the labeled convex polytopes X and Y for v_0 and v_1 respectively are fundamental domains of the lattice L associated to the edge e . Then, we can translate almost every point in X to Y by a unique vector in the lattice L . Therefore, each closed path based on a vertex v_0 in G corresponds to a PET on X . The resulting system is called the multigraph PETs. The construction is considered functorial: there is a functor from the the fundamental group $\pi_1(G, x)$ based on a vertex x to the group of PETs defined on the labeled convex polytope X of x , i.e.

$$\pi_1(G, x) \rightarrow \text{PET}(X).$$

1.3. Triple Lattice PETs. In this section, we describe the construction of triple lattice PETs whose corresponding multigraph are triangles. Let F_0 be a parallelogram determined by the vectors $(2, 0)$ and $(s, \sqrt{3}s)$ for $s \in [0, 1)$. Let r_0, r_1 and r_2 be the reflections about the lines in the directions of cubic roots of unity passing through the origin. Let D_6 be the dihedral group of order 6 generated by the reflections r_0, r_1 and r_2 . The 6 parallelograms in Figure 1 are in the orbit of F_0 under the dihedral group D_6 . Let F_i be the parallelogram centered at the origin and translation equivalent to the one labeled as F_i in Figure 1 for $i \in \{0, 1, 2\}$. Let L_i be the lattice generated by the vectors which are the sides of the parallelogram labeled by L_i in Figure 1 for $i \in \{0, 1, 2\}$.

We will verify the fact that F_i and $F_{(i+1) \bmod 3}$ are fundamental domains of the lattice L_i in the later section. It follows that for almost every point $p \in F_i$, there exists a unique vector $V_p \in L_i$ such that $p + V_p \in F_{(i+1) \bmod 3}$. To define the triple lattice PETs, we consider the set $X'_s = \bigcup_{i=0}^2 F_i$. Given $p \in F_i$, define the map

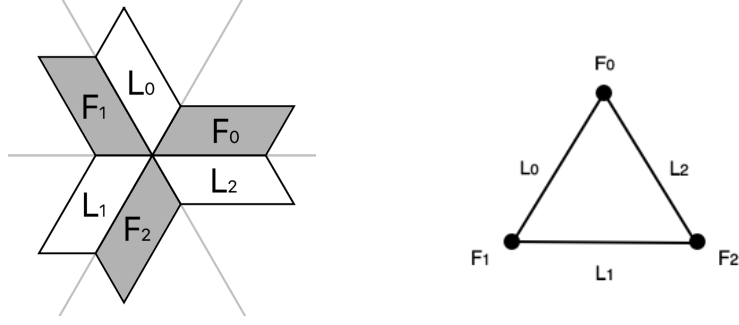


FIGURE 1. The scheme for the triple lattice PETs

$g_s : X'_s \rightarrow X'_s$ by the formula:

$$g_s(p) = p + V_p \in F_{(i+1) \bmod 3}, \quad V_p \in L_i.$$

We leave g undefined on the point p when V_p is not uniquely determined by p .

Definition 1.6. Let $X_s = F_0$. The *triple lattice PET* is given by the map $f'_s : X_s \rightarrow X_s$ such that

$$f'_s = (g_s)^3.$$

We denote the system by (X_s, f'_s) .

In order to obtain symmetries, we introduce a *cut-and-paste* operation (Section 2.2) which can be seen as a simple rearrangement of the map f'_s (Figure 2). We call the the resulting system after cut-and-paste the triple lattice PETs denoted by (X_s, f_s) .

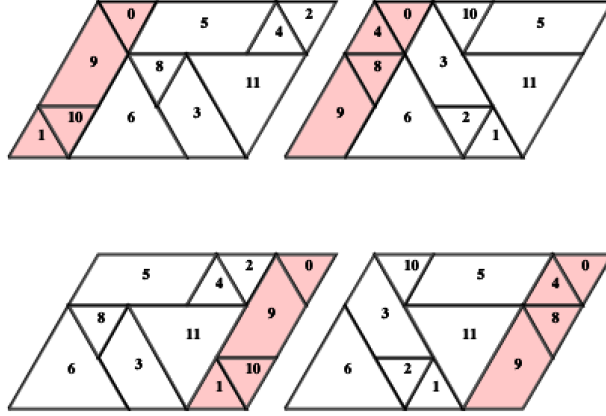


FIGURE 2. An illustration of the cut-and-paste operation on X_s for $s = 3/4$. The top figures show the partitions \mathcal{A}' and \mathcal{B}' for the triple lattice PET f'_s . The bottom figure show the modified partitions \mathcal{A} and \mathcal{B} for the map f_s obtained by translating all the elements of \mathcal{A}' and \mathcal{B}' in the red parallelograms to the right and then move the resulting parallelogram centered at the origin again.

1.4. **Main Results.** Let $R_1, R_2 : (0, 1) \rightarrow (0, 1)$ be the maps given by

$$R_1(s) = \frac{s}{1 + s - s\lfloor 1/s \rfloor} \quad \text{and} \quad R_2(s) = \frac{1-s}{s}.$$

We define the renormalization map $R : (0, 1) \rightarrow (0, 1)$ as follows

$$R(s) = \begin{cases} R_1(s) & \text{if } s \in (0, \frac{1}{2}), \\ R_2(s) & \text{if } s \in [1/2, 2/3), \\ R_1R_2(s) & \text{if } s \in [2/3, 1). \end{cases}$$

Theorem 1.7 (Renormalization). *Let $s \in (0, 1)$ and $t = R(s)$. There exists a subset Y_s such that the first return map $f_s|_{Y_s} : Y_s \rightarrow Y_s$ satisfies*

$$f_s|_{Y_s} = \psi_s^{-1} \circ f_t \circ \psi_s.$$

where ψ_s is the map of similarity such that $Y_s \mapsto X_t$.

The renormalization theorem allows us to deduce corollaries on the limit set Λ_ϕ for $\phi = \frac{\sqrt{5}-1}{2}$. Note that ϕ is the only fixed point under the renormalization map R . The limit set Λ_ϕ can be obtained by a sequence of substitutions on the isosceles trapezoids A, B and C in X_ϕ as shown Figure 6-9.

Theorem 1.8. *The limit set Λ_ϕ is the limit of embedded polygons in \mathbb{R}^2 .*

The substitutions generate an iterated function system of similarities, and the limit set Λ_ϕ is a self-similar set. We compute the Hausdorff dimension of Λ_ϕ .

Theorem 1.9. *The Hausdorff dimension of the limit set Λ_ϕ satisfies the property:*

$$\dim_H(\Lambda_\phi) = \frac{\log(-1 + \sqrt{2})}{\log \phi} = 1.83147\dots < 2.$$

Corollary 1.10. *The limit set Λ_ϕ has Lebesgue measure zero.*

1.5. **Outline.** In Section 2, we provide basic definitions and properties related to the triple lattice PETs. Properties of the renormalization map R are discussed in this section.

Section 3 introduces the fiber bundle method which is a key tool to prove the main theorem.

In Section 4, we prove the Renormalization Theorem using two inductions on the parameter space.

Symmetries of the triple lattice map f_s are discussed in Section 5.

In Section 6, we study the limit set Λ_ϕ following a description of the substitution rule on the isosceles trapezoids. We use the substitution to compute the Hausdorff dimension and Lebesgue measure of the limit set Λ_ϕ .

All computational data are provided in Section 7.

1.6. **Acknowledgement.** The author would like to thank her advisor Professor Richard Schwartz for his constant support, encouragement and guidance throughout this project. The author would also like to thank Patrick Hooper and Yuhan Wang for helpful suggestions at different steps of the paper.

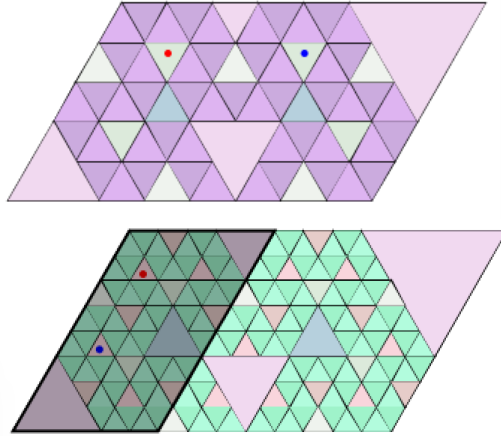


FIGURE 3. The top figure is an illustration of f_t for $t = 5/8 = R(8/13)$. Given a point (red) in X_t , its image is shown blue. The figure on bottom shows Y_s (lightly shaded) for $s = 8/13$. The image of the given point (red) under the first return $f_s|_{Y_s}$ is shown in blue. The first return map $f_s|_{Y_s}$ is conjugate to f_t by a similarity.

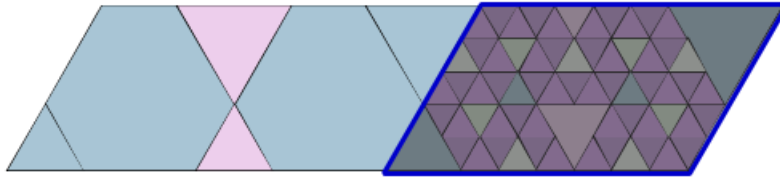


FIGURE 4. Y_s lightly shaded for $s = 5/18$ and $R(5/18) = 5/8$

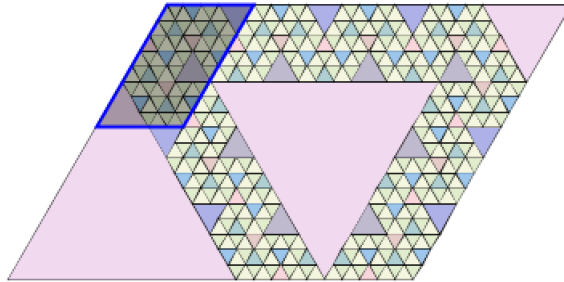


FIGURE 5. Y_s lightly shaded for $s = 18/23$ and $R(18/23) = 5/8$

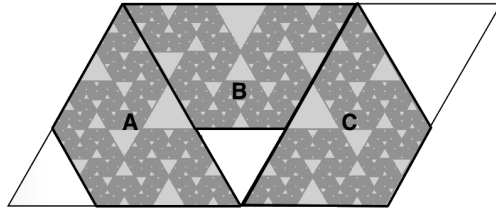


FIGURE 6. Isosceles trapezoids A, B, C in X_ϕ

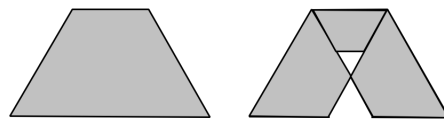


FIGURE 7. Substitution rule of the isosceles trapezoids

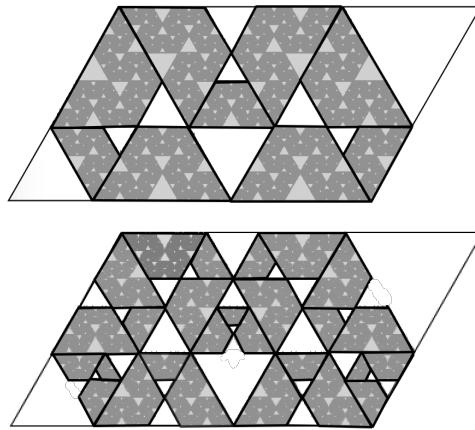


FIGURE 8. The iterations of the substitution rule on trapezoids A, B and C

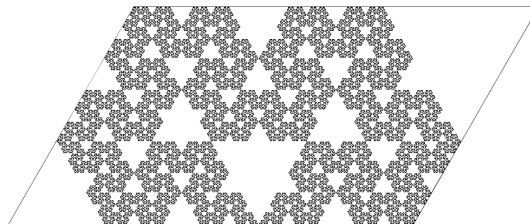


FIGURE 9. The limit set Λ_ϕ

2. PRELIMINARIES

2.1. Fundamental Domains. We check the fact that each parallelogram F_i is a fundamental domain of L_i and $L_{(i-1) \bmod 3}$ for $i \in \{0, 1, 2\}$. According to [17], it is sufficient to check two facts:

- (1) The parallelogram F_i and the lattice quotient \mathbb{R}^2/L_i or $\mathbb{R}^2/L_{(i-1) \bmod 3}$ have the same volume. It is easy to see that

$$\text{Area}(\mathbb{R}^2/L_j) = \text{Area}(F_i) = 2\sqrt{3}s.$$

for $i \in \{0, 1, 2\}$.

- (2) The union

$$\bigcup_{V \in L} (F_i + V)$$

provides a tiling of \mathbb{R}^n where $L = L_i$ or $L = L_{(i-1) \bmod 3}$ for $i \in \{0, 1, 2\}$.

Here we only discuss the case when $i = 0$. The same argument can be applied similarly by reflections. Recall that the lattice L_0 is generated by the vectors

$$V_0 = s(1, \sqrt{3}) \quad \text{and} \quad V_1 = (-1, \sqrt{3}).$$

and F_0 is a parallelogram determined by the vectors $s(1, \sqrt{3})$ and $(2, 0)$. First we notice that F_0 and $F_0 + V_0$ form adjacent tiles meeting at the top side of F_0 . Consider a band \mathcal{S} between lines $l_1 : y = \sqrt{3}x$ and $l_2 : y = \sqrt{3}(x - 2)$. The union $\bigcup_{m \in \mathbb{Z}} (F_0 + mV_0)$ form a tiling of \mathcal{S} in \mathbb{R}^2 . Notice

that by applying V_1 , the band \mathcal{S} translates to the adjacent band $\mathcal{S} - (2, 0)$. Therefore, the union $\bigcup_{m, n \in \mathbb{Z}} (F_0 + mV_0 + nV_1)$ is a tiling in \mathbb{R}^2 .

Similarly, the lattice L_2 is generated by the vectors $V_0 = (2, 0)$ and $V_1 = s(1, -\sqrt{3})$. The union $\bigcup_{m \in \mathbb{Z}} F_0 + mV_0$ form a tiling in the band \mathcal{S} between the horizontal axis and $y = \sqrt{3}s$. Moreover, The vector V_1 translates \mathcal{S} to $\mathcal{S} + (0, \sqrt{3})s$. Consequently, the union $\bigcup_{m, n \in \mathbb{Z}} (F_0 + mV_0 + nV_1)$ is a tiling in \mathbb{R}^2 .

2.2. Cut-and-Paste Operation. In this section, we explain the cut-and-paste operation in detail. Suppose that $s \in (0, 1)$. Let a_1 be the first non-zero integer of the continued fraction expansion of s , i.e.

$$a_1 = \lfloor 1/s \rfloor.$$

Let $\mathcal{A}', \mathcal{B}'$ be the partitions of X_s defining a triple lattice PET f'_s . Let $Y_s \subset X_s$ be a parallelogram (shown as red in the top figure) such that Y_s and X_s share the same lower left vertex v . The sides of Y_s are determined by the vectors

$$v + (s, \sqrt{3}s) \quad \text{and} \quad v + (2 - 2a_1s, 0),$$

The cut-and-paste operation \mathcal{OP} on the parallelogram X_s can be described as follows: for each point $p \in X_s$, if $p \in Y_s$, then we translate p by the vector $(2 - 2a_1s, 0)$. Otherwise, translate p by $(-2a_1s, 0)$. Note that X_s remains the same after the operation \mathcal{OP} . We obtain the modified partitions \mathcal{A} and \mathcal{B} on X_s which produce a new family of PETs $f_s : X_s \rightarrow X_s$.

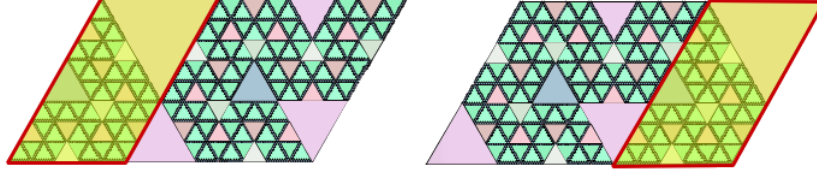


FIGURE 10. The figure on the left shows the periodic pattern Δ'_s of the map f'_s before the cut-and-paste operation \mathcal{OP} and the figure on the right shows the Δ_s of f_s after \mathcal{OP} .

2.3. Algorithm for generating Periodic Tiles. Let $\mathcal{A}_0 = \{A_i\}_{i=1}^m$ and $\mathcal{B}_0 = \{B_i\}_{i=1}^m$ be the partitions of polygons such that the map f_s is determined by \mathcal{A}_0 and \mathcal{B}_0 . For integers $n \geq 1$, we inductively define \mathcal{A}_n to be the collection of polygons

$$f^{-n}(f^n(P) \cap A_i), \quad P \in \mathcal{A}_{n-1} \text{ and } A_i \in \mathcal{A}_0.$$

The partition \mathcal{A}_n is a refinement of \mathcal{A}_{n-1} . For each $n \geq 2$, the iteration f^n is not defined on

$$\bigcup_{P \in \mathcal{A}_n} \partial P.$$

Let $P \in \mathcal{A}_n$ be an open polygon. Every point in P must have the same codings. It follows that if a point $p \in P$ is periodic of period n , then all points of P are periodic with period n . Remark that each periodic tile is convex because of the fact that intersections of convex polygons are convex.

2.4. Renormalization Map. We discuss the properties of the renormalization map $R : (0, 1) \rightarrow (0, 1)$ defined in section 1.7 through continued fraction expansions. Suppose that $s \in (0, 1)$ is rational and has continued fraction expansion (c.f.e)

$$(0; a_1, a_2, \dots, a_n).$$

If $s \in (0, \frac{1}{2})$, then $a_1 \geq 2$ in the c.f.e of s . The renormalization map R has the action

$$(0; a_1, a_2, \dots, a_n) \mapsto (0; 1, a_2, \dots, a_n).$$

For example, $5/23 = (0; 4, 1, 1, 2)$ and $R(5/23) = \frac{5}{8} = (0; 1, 1, 1, 2)$.

If $s \in [1/2, 2/3)$, then its c.f.e. can be written in the form of $(0; 1, 1, \dots, a_n)$. The renormalization map R can be viewed as a shift on the fractional part of the c.f.e., i.e.

$$(0; 1, 1, a_3, \dots, a_n) \mapsto (0; 1, a_3, \dots, a_n).$$

The parameter $\phi = \frac{-1+\sqrt{5}}{2} = (0; 1, 1, \dots)$ is the only fixed point under the renormalization map R .

If $s \in [2/3, 1)$, then $a_1 = 1$ and $a_2 \geq 2$ in the c.f.e.. The map R first shift the fractional part of the c.f.e. to the right, and then reduce a_2 to 1, i.e.

$$(0; 1, a_2, \dots, a_n) \mapsto (0; 1, a_3, \dots, a_n).$$

Therefore, the renormalization map R has the action

$$\left(\frac{n-1}{n}, \frac{n}{n+1}\right) \mapsto \left(\frac{1}{2}, 1\right) \quad \text{and} \quad \left(\frac{1}{n}, \frac{1}{n-1}\right) \mapsto \left(\frac{1}{2}, 1\right).$$

Moreover, when s is irrational, all arguments hold true by taking $n \rightarrow \infty$.

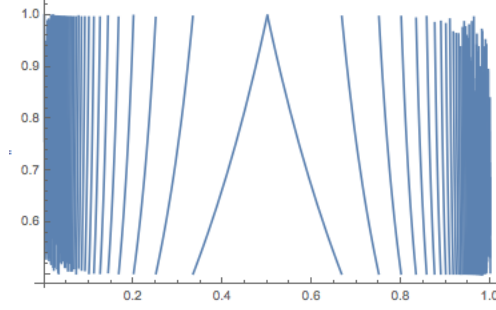


FIGURE 11. The plot of renormalization map R with range $[\frac{1}{2}, 1]$

2.5. Hausdorff dimension. In this section, we provide basic definitions related to Hausdorff dimension and a formula to calculate it (see [5] for reference).

Definition 2.1. Suppose that F is a compact set of \mathbb{R}^n and $s \geq 0$. Define

$$H_\delta^s(F) = \inf \left\{ \sum_{i=1}^{\infty} \text{diam}(U_i)^s \mid \text{diam}(U_i) \leq \delta \text{ and } F \subset \bigcup_{i=1}^{\infty} U_i \right\}.$$

The *Hausdorff measure* is defined to be the limit

$$H^s(F) = \lim_{\delta \rightarrow 0} H_\delta^s(F).$$

There is a critical value s_0 of s at which H^s jumps from ∞ to 0. The value s_0 is called *Hausdorff dimension*. Formally, the Hausdorff dimension $\dim_H F$ of a compact set F is defined as follows:

Definition 2.2.

$$\dim_H F = \inf \{s \geq 0 : H^s(F) = 0\} = \sup \{s : H^s(F) = \infty\}.$$

If $s = \dim_H F$, then $0 < H^s(F) < \infty$.

Here we state a classical result in [5] to compute Hausdorff dimensions of self-similarity sets. Let $\{\sigma_0, \sigma_1, \dots, \sigma_m\}$ be a set of similarities with scaling ratios $0 < c_i < 1$ for $1 \leq i \leq m$. If the following conditions are satisfied:

- (1) attractor condition: the set F is an attractor i.e.

$$F = \bigcup_{i=1}^m \sigma_i(F),$$

- (2) open set condition: there exists non-empty bounded open set V such that

$$V \supset \bigcup_{i=1}^m \sigma_i(V),$$

then the Hausdorff dimension $\dim_H F = s$, where s is given by

$$\sum_{i=1}^m c_i^s = 1.$$

2.6. Computer Assistance. We give a proof for the main renormalization theorem and symmetrical properties of periodic patterns (see Section 3 and 4) for the map f_s with computer assistance. The proof involves calculations to determine if a given pair of polyhedra are nested or disjoint. We scale all the convex polyhedra so that all the calculations are done in integers or half integers. Hence, there is no roundoff error. The pictures of partitions, periodic patterns and limit sets are taken from my java program. The program also do all the calculations. The program can be downloaded from the URL

https://www.math.brown.edu/~renyi/triple_lattice/project.html

3. THE FIBER BUNDLE PICTURE

Suppose $s \in (0, 1)$ and $t = R(s)$. We want to show the first return map $f_s|_{Y_s}$ conjugates to the map f_t by a map of similarity ψ_s . Since it is impossible to apply calculations on every $s \in (0, 1)$, the idea of the proof is to reduce all the calculations to finitely many computations on the fiber bundle \mathcal{X} which is a convex polyhedron in \mathbb{R}^3 .

The construction is inherited from [16] in Chapter 26. Define $\mathcal{X} \in \mathbb{R}^3$ as follows

$$\mathcal{X} = \{(x, y, s) | (x, y) \in X_s, s \in [\frac{1}{2}, 1]\}.$$

The set \mathcal{X} is a convex polyhedron and a fiber bundle over $[1/2, 1)$ such that the fiber above s is the parallelogram X_s . Let $F : \mathcal{X} \rightarrow \mathcal{X}$ be the fiber bundle map given by the formula:

$$F(x, y, s) = (f_s(x, y), s).$$

It is easy to see that F is a piecewise affine map. It is because for each $(x, y) \in X_s$, the map f_s is of the format

$$f_s(x, y) = (x, y) + (m_0s + m_1, (n_0s + n_1)\sqrt{3})$$

where $m_i, n_i \in \mathbb{Z}$ for $i = 0, 1$. If we vary the point (x, y) and the parameter s in a small neighborhood, the integers m_i, n_i for $i = 1, 2$ will not change.

Definition 3.1. A *maximal domain* of \mathcal{X} is a maximal subset in \mathcal{X} where the fiber bundle map F is entirely defined and continuous.

In other words, a maximal domain D of \mathcal{X} is a maximal subset of \mathcal{X} such that for all $(x, y, s) \in \text{Int}(D)$, the fiber bundle map $F : \mathcal{X} \rightarrow \mathcal{X}$ is in the form of

$$F(x, y, s) = (x, y, s) + (m_0s + m_1, y + (n_0s + n_1)\sqrt{3}, 0)$$

for the fixed integers m_i, n_i where $i = 0, 1$. It follows that for each maximal domain D , there is a 4-tuple (m_0, m_1, n_0, n_1) encoded the information of its translation vector. We call it the *coefficient tuple* of the maximal domain D .

The fiber bundle \mathcal{X} is partitioned into 12 maximal domains D_i for $i = 0, \dots, 11$. The vertices of the maximal domains are of the form

$$\left(\frac{1}{2}\frac{a}{q}, \frac{\sqrt{3}}{2}\frac{b}{q}, \frac{p}{q}\right), \quad \text{for } a, b, p, q \in \mathbb{Z}$$

and

$$(p, q) \in \{(1, 2), (2, 3), (1, 1)\}.$$

The list of maximal domains along with their coefficient tuple is provided in Section 7.

- Remark 3.2.** (1) All maximal domains except for D_7 have at least one vertices with z -coordinate greater than $2/3$. Formally, we consider the subset $\mathbb{E} = \{(x, y, z) : z \geq 2/3\}$ of \mathbb{R}^3 . For $i = 0, \dots, 12$, the Lebesgues measure $\mu(D_i \cap \mathbb{E})$ equals to 0 when $i = 7$ and strictly greater than 0 otherwise. We say D_7 *degenerates* on the interval $[2/3, 1)$.
- (2) The union of cross sections obtained by intersecting the maximal domains and the plane $z = s$ gives a partition \mathcal{A} on X_s which determines the triple lattice map f_s .

4. PROOF OF THE RENORMALIZATION THEOREM

4.1. Outline of the Proof. The proof of the renormalization theorem relies on two inductions. We provide an outline here.

- We first show that the main theorem holds true when $s \in [\frac{1}{2}, \frac{2}{3})$ by applying calculations on 12 maximal domains in the fiber bundle \mathcal{X} .
- By the similar technique, we check the renormalization theorem on the two other base cases when $s \in [2/3, 3/4)$ and $s \in [\frac{3}{4}, \frac{4}{5})$.
- We apply Induction I on the intervals of the format $[\frac{n-1}{n}, \frac{n}{n+1})$ for $n \geq 2$ to show that Theorem 1.7 holds true for all $s \in [\frac{1}{2}, 1)$. More precisely, we find that for $s \in [\frac{n-1}{n}, \frac{n}{n+1})$, the first return map $f_s|_{Y_s}$ is similar to $f_t|_{Y_t}$ for some $t \in [\frac{n}{n+1}, \frac{n+1}{n+2})$. Therefore, we have renormalization scheme proved on the intervals

$$[\frac{3}{4}, \frac{4}{5}) \mapsto [\frac{4}{5}, \frac{5}{6}) \mapsto [\frac{5}{6}, \frac{6}{7}) \mapsto \dots$$

By taking the union

$$\bigcup_{n \geq 2} [\frac{n-1}{n}, \frac{n}{n+1}) = [\frac{1}{2}, 1),$$

Theorem 1.7 can be shown for $s \in [\frac{1}{2}, 1)$.

- We apply induction II to verify Theorem 1.7 when the parameter $s \in [\frac{1}{n}, \frac{1}{n-1})$ for all $n \geq 2$. We show that the periodic pattern for $s \in [\frac{1}{n}, \frac{1}{n-1})$ and $t \in [\frac{1}{n+1}, \frac{1}{n})$ are same up to scaling and adding on one central parallelogram. By this observation, we have renormalization scheme proved on the intervals

$$[\frac{1}{2}, 1) \mapsto [\frac{1}{3}, \frac{1}{2}) \mapsto [\frac{1}{4}, \frac{1}{3}) \mapsto \dots$$

Consequently, the renormalization theorem is shown for $s \in (0, 1)$ that is the union

$$\bigcup_{n \geq 2} [\frac{1}{n}, \frac{1}{n-1}) = (0, 1).$$

4.2. Base Case 1. Suppose $s \in I_0 = [1/2, 2/3)$ and $t = R(s) \in (\frac{1}{2}, 1]$. Now we define Y_s (Figure 12) which is the set for the first return map. Let $Y_s \subset X_s$ be the parallelogram determined by the vectors

$$V_0 + (s, \sqrt{3}s), \quad \text{and} \quad V_0 + (2 - 2s, 0).$$

where $V_0 = (-\frac{s}{2} - 1, -\frac{\sqrt{3}s}{2})$ is the lower left vertex of X_s .

Before giving the explicit formula, we give an informal description of the similarity ψ_s in Theorem 1.7 mapping Y_s to X_t . The map ϕ_s first translates the set Y_s to

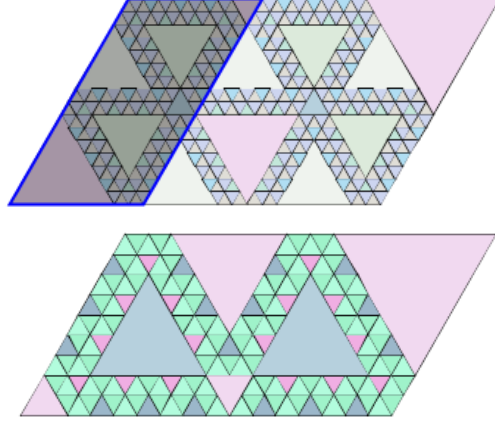


FIGURE 12. Y_s (lightly shaded) for $s = \frac{16}{25}$ and Δ_t for $t = R(s) = \frac{9}{16}$

center at the origin. Then, rotate the obtained parallelogram Y_s counterclockwise by $2\pi/3$ around the origin. Flip the obtained shape about the horizontal axis. Finally, scale the resulting parallelogram by $1/s$. Hence, the formula of $\psi_s : Y_s \rightarrow X_t$ for $s \in I_0$ is given as follows:

$$\begin{bmatrix} x \\ y \end{bmatrix} \mapsto \frac{1}{s} \begin{bmatrix} -1/2 & -\sqrt{3}/2 \\ -\sqrt{3}/2 & 1/2 \end{bmatrix} \begin{bmatrix} x+s \\ y \end{bmatrix}.$$

Define the polyhedron $\mathcal{Y} \subset \mathcal{X}$ as follows

$$\mathcal{Y} = \{(x, y, s) | (x, y) \in Y_s, s \in I_0\}.$$

The polyhedron \mathcal{Y} is a fiber bundle over I_0 such that the fiber above s is the parallelogram Y_s . We define the affine map $\Psi : \mathcal{Y} \rightarrow \mathcal{X}$ by piecing together all the similarities ψ_s for $s \in I_0$

$$\Psi(x, y, s) = \left(\psi_s(x, y), R(s) \right).$$

Note that the map R has the action that

$$I_0 = [1/2, 2/3] \mapsto (1/2, 1].$$

The inverse map Ψ^{-1} is given by the formula:

$$\Psi^{-1}(x, y) = \left(\psi_s^{-1}(x, y), \frac{1}{1+s} \right).$$

Here we give the main calculation steps of the proof. For each maximal domain D_i in \mathcal{X} , we check the following properties by computer:

- (1) There exists an integer $n > 0$ such that

$$F^n \circ \Psi^{-1}(D_i) \subseteq \mathcal{Y}$$

and

$$F^k \circ \Psi^{-1}(D_i) \cap \mathcal{Y} = \emptyset, \quad \text{for all } 0 \leq k < n.$$

It means that the first return map on \mathcal{Y} is well-defined and the fiber bundle map F returns to the polyhedron \mathcal{Y} as F^n .

- (2) $F^n \circ \Psi^{-1}(D_i) \subseteq \Psi^{-1} \circ F(D_i)$

(3) Pairwise disjointness: set $M_i = F^n \circ \Psi^{-1}(D_i)$.

$$\text{Int}(M_i) \cap \text{Int}(M_j) = \emptyset \quad \text{for } i \neq j.$$

(4) Filling:

$$\sum_{i=0}^{11} \text{Volume}(M_i) = \text{Volume}(\mathcal{Y}).$$

The above computation shows that the first return map $F|_{\mathcal{Y}}$ on \mathcal{Y} satisfies the equation

$$F|_{\mathcal{Y}} = \Psi^{-1} \circ F \circ \Psi.$$

Therefore, the renormalization theorem on the first base case $I_0 = [1/2, 2/3)$ has been proved. \square

4.3. Base case 2 and 3. Consider $I_1 = [2/3, 3/4)$ and $I_2 = [3/4, 4/5)$. Suppose $s \in [2/3, 3/4)$ or $[3/4, 4/5)$. In these cases, we want to apply the similar proof as the one in the previous section. One difference is that the subset Y_s is chosen differently than before. We define the subset $Y_s \subset X_s$ for $s \in I_j$ for $i = 1, 2$ as follows. Suppose $s \in I_j$ for $j \in \{1, 2\}$. Let $V_0 = (\frac{s}{2} - 1, \frac{\sqrt{3}s}{2})$ be the top left vertex of X_s . Consider a parallelogram Y_s determined by the vectors

$$V_0 + (2a_s, 0) \quad \text{and} \quad V_0 - b_s(1, -\sqrt{3})$$

where

$$a_s = 1 - s \quad \text{and} \quad b_s = 1 - \lfloor \frac{s}{a_s} \rfloor a_s.$$

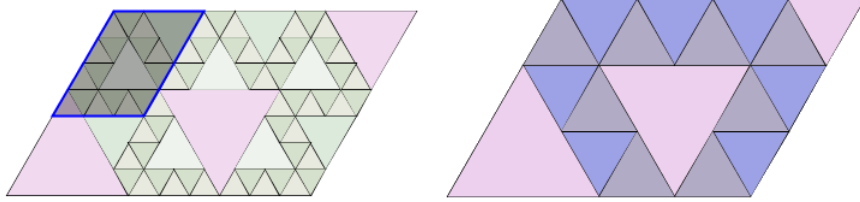


FIGURE 13. Y_s (lightly shaded) for $s = 7/10$ and Δ_t for $t = R(s) = 3/4$

Here we show that the renormalization theorem holds true for $s \in I_1$ and $s \in I_2$.

Lemma 4.1. *Suppose $s \in I_j$ and $t = R(s)$ for $j \in \{1, 2\}$. The first return map $f_s|_{Y_s}$ on Y_s conjugates to f_t by a map of similarity ψ_s .*

We want to use the argument as the one in the previous section. Similarly, we define the polyhedron $\mathcal{Y}(I_j)$ as a subset of \mathcal{X} over the interval I_j , i.e.

$$\mathcal{Y}(I_j) = \{(x, y, s) | (x, y) \in Y_s, s \in I_j\} \quad \text{for } j = 1, 2.$$

Suppose $s \in I_j$ and $t = R(s) \in (1/2, 1]$. The map of similarity $\psi_s : Y_s \rightarrow X_t$ is defined similarly as the in the Section 3.1 but with a different scaling factor $1/b_s$

for $b_s = (j + 1)s - j$. Let $s \in I_j$ for $j \in \{1, 2\}$, the formula of $\psi_s : Y_s \rightarrow X_t$ is given by the following formula:

$$\begin{bmatrix} x \\ y \end{bmatrix} \mapsto \frac{1}{(j + 1)s - j} \begin{bmatrix} -1/2 & -\sqrt{3}/2 \\ -\sqrt{3}/2 & 1/2 \end{bmatrix} \begin{bmatrix} x - \frac{j-(j+3)s}{4} \\ y - \frac{\sqrt{3}j(1-s)}{4} \end{bmatrix}$$

The affine map $\Psi : \mathcal{Y}(I_j) \rightarrow \mathcal{X}$ and its inverse Ψ^{-1} are given by

$$\Psi(x, y, s) = (\psi_s(x, y), R(s)), \quad \Psi^{-1}(x, y, s) = (\psi_s^{-1}(x, y), \frac{1 + sj}{1 + s(j + 1)}).$$

By following the same computation in base case 1, we verify the renormalization theorem for $s \in I_1$ and I_2 .

4.4. Induction I. Consider the map $T : [2/3, 1) \rightarrow [1/2, 1)$ given by

$$T(s) = \frac{2s - 1}{s}$$

and its inverse map

$$T^{-1}(s) = \frac{1}{2 - s}.$$

The map T^{-1} has action

$$\left[\frac{3}{4}, \frac{4}{5}\right) \mapsto \left[\frac{4}{5}, \frac{5}{6}\right) \mapsto \dots \mapsto \left[\frac{n-2}{n-1}, \frac{n-1}{n}\right) \mapsto \left[\frac{n-1}{n}, \frac{n}{n+1}\right) \mapsto \dots$$

It follows that

$$\left[\frac{1}{2}, 1\right) = \left[\frac{1}{2}, \frac{2}{3}\right) \cup \left[\frac{2}{3}, \frac{3}{4}\right) \cup \bigcup_{k=0}^{\infty} T^{-k} \left[\frac{3}{4}, \frac{4}{5}\right).$$

Lemma 4.2 (Induction I). *If the Theorem 1.7 is true for $t \in [\frac{n-1}{n}, \frac{n}{n+1})$ for $n \geq 4$, then it also holds for $s = T^{-1}(t) \in [\frac{n}{n+1}, \frac{n+1}{n+2})$.*

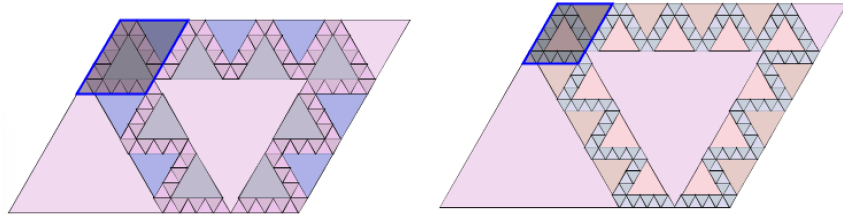


FIGURE 14. Y_t for $t = 13/17$ and Y_s for $s = T^{-1}(t) = 17/21$

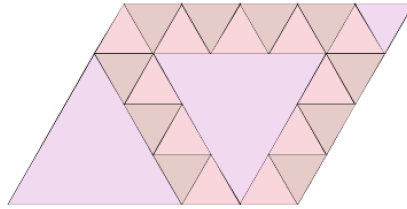


FIGURE 15. Δ_u for $u = R(s) = R(t) = 4/5$

It is equivalent to prove that the following diagram commutes.

$$\begin{array}{ccc} Y_s & \xrightarrow{f_s|_{Y_s}} & Y_s \\ \downarrow \xi_s & & \downarrow \xi_s \\ Y_t & \xrightarrow{f_t|_{Y_t}} & Y_t \end{array}$$

The map ξ_s is a homothety (scaling and translation) with the scaling ratio $1/s$ such that $Y_s \mapsto Y_t$. The explicit formula of ξ_s is given by

$$\xi_s(x, y) = \frac{1}{s}(x - x_s, y - y_s) + (x_t, y_t),$$

where $(x_s, y_s) = (\frac{s}{2} - 1, \frac{\sqrt{3}s}{2})$ is the top left vertex of X_s and the point (x_t, y_t) is defined similarly.

The idea of the proof is to modify the map f_s in order to shorten the return time for the point $p \in Y_s$, and then show that the modified map of f_s is conjugate to the map f_t via a similarity. Therefore, the statement of the first return map follows directly. To see this, we parametrize each element of the partition \mathcal{A}_s and its translation vector.

Proof. Let $\mathcal{A}_s = \{A_i(s)\}_{i=1}^m$ be a partition on X_s which determine the map f_s and $V_s = \{V_i(s)\}_{i=1}^m$ be a set of translation vectors such that

$$f_s(x) = x + V_i(s) \quad \text{for } x \in \text{Int}(A_i).$$

According to previous section, we already know that there are 12 maximal domains D_i in the fiber bundle \mathcal{X} over the interval $[1/2, 1)$ and the maximal domain D_7 degenerates on the interval $[2/3, 1)$. It follows that, there are 11 elements $A_i(s)$ for the partition \mathcal{A}_s for $s \in [2/3, 1)$. We parametrize these 11 maximal domains D_i and their translation vectors V_i by the parameter $s \in (2/3, 1)$ for $i = \{0, 1, \dots, 11\}$ and $i \neq 7$.

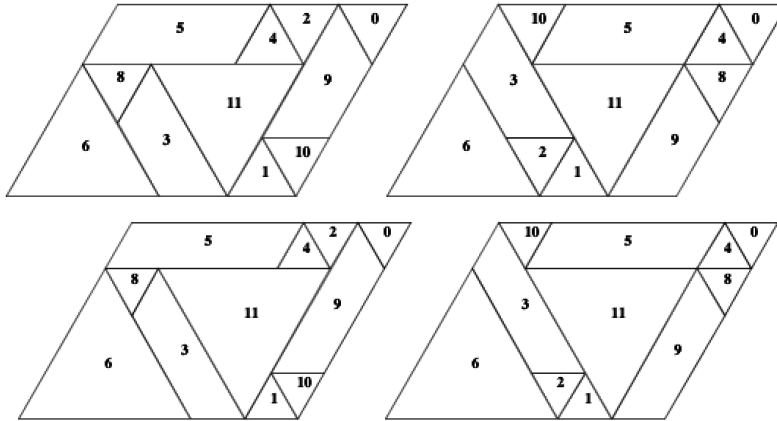


FIGURE 16. The partition \mathcal{A}_t and \mathcal{B}_t of the triple lattice PET f_s for $t = 13/17$ (top); The partition \mathcal{A}_s and \mathcal{B}_s of the triple lattice PET f_s for $s = 17/21$ (bottom);

Let $(m_0, m_1, n_0, n_1) \in \mathbb{Z}^4$ be a coefficient tuple of a maximal domain D_i in \mathcal{X} (Section 3). Recall that for every point $(x, y, s) \in D_i$,

$$F(x, y, s) = (x, y, s) + (m_0s + m_1, (n_0s + n_1)\sqrt{3}, 0).$$

Let

$$a_s = 1 - s \quad \text{and} \quad b_s = s - a_s = 2s - 1.$$

Note that

$$\begin{aligned} a_t = 1 - t = 1 - \frac{2s - 1}{s} &\Rightarrow a_t = \frac{a_s}{s}, \\ b_t = 2t - 1 = \frac{3s - 2}{s} &\Rightarrow b_t = \frac{b_s - a_s}{s}. \end{aligned}$$

According to the translation vectors (or coefficient tuples), we can divide the elements $A_i(s) \in \mathcal{A}_s$ for $i = \{0, 1, \dots, 11\}$ and $i \neq 7$ into three different classes:

- (1) The element $A_i(s)$ is fixed. When $i = 0, 6, 11$, the set $A_i(s)$ is a trivial periodic tile given by the map f_s . Each $A_i(s)$ is an equilateral triangle. The parametrization of each triangle is listed below:

$$A_0(s) : \quad v = \left(\frac{1}{2}s + 1, \frac{\sqrt{3}}{2}s\right), \quad v - (2a_s, 0), \quad v - a_s(1, \sqrt{3}),$$

$$A_6(s) : \quad v = \left(-\frac{1}{2}s - 1, -\frac{\sqrt{3}}{2}s\right), \quad v + (2b_s, 0), \quad v + b_s(1, \sqrt{3}),$$

$$A_{11}(s) : \quad v = \left(-\frac{1}{2}s, \left(-\frac{3}{2}s + 1\right)\sqrt{3}\right), \quad v + (2b_s, 0), \quad v + b_s(1, \sqrt{3}).$$

We restrict our attention on the parametrization of the elements in \mathcal{A}_s which belongs to the subset

$$\bar{X}_s = X_s \setminus \bigcup_{i=0,6,11} A_i(s).$$

- (2) For $i \in \{1, 4\}$, the translation vector $V_i(s)$ of $A_i(s)$ are of the form $2a_1\omega$ for ω is a unit vector in the direction of cubic root of unity.

$$V_1(s) = a_s(s)(2, 0) \quad \text{and} \quad V_4(s) = -a_s(2, 0).$$

The element $A_i(s)$ are equilateral triangles of side length $2a_s$.

$$A_1 : \quad v_0 = \left(\frac{1}{2}s + 1, \frac{\sqrt{3}}{2}s\right), \quad v_0 + (2a_s, 0), \quad v_0 + a_s(1, \sqrt{3}).$$

$$A_4 : \quad v_0 = \left(\frac{7}{2}s - 2, \left(\frac{3}{2}s - 1\right)\sqrt{3}\right), \quad v_0 + (2a_s, 0), \quad v_0 + a_s(1, -\sqrt{3}).$$

Since $a_i(t) = \frac{1}{s}a_i(s)$, we have

$$V_i(t) = \frac{1}{s}V_i(s),$$

and $A_i(s), A_i(t)$ are same up to similarity with a scaling factor $1/s$.

- (3) For $i \in \{2, 8, 10\}$, let Λ_s be the lattice generated by the sides of the parallelogram X_s . The translation vector $V_i(s)$ are of the form $2a_s\omega \pmod{\Lambda_s}$ where ω is a vector in the direction of cubic root of unity. More precisely,

$$V_2(s) = a_s(-1, \sqrt{3}) \pmod{\Lambda_s}, \quad V_8(s) = a_s(-2, 0) \pmod{\Lambda_s}$$

$$V_{10}(s) = a_s(-1, -\sqrt{3}) \pmod{\Lambda_s}.$$

Therefore,

$$V_i(t) = \frac{1}{s}V_i(s), \quad \text{for } i = 2, 8, 10.$$

Each $A_i(s)$ is an equilateral triangle with a top horizontal side. The side length of each triangle is $2a_s$. The top left vertex u_i of $A_i(s)$ is provided here:

$$u_2 = \left(\frac{5}{2}s - 1, \frac{\sqrt{3}}{2}s\right), \quad u_8 = \left(\frac{3}{2}s - 2, \left(\frac{3}{2}s - 1\right)\sqrt{3}\right), \quad u_{10} = \left(\frac{1}{2}s, \left(-\frac{3}{2}s + 1\right)\sqrt{3}\right).$$

- (4) For $i \in \{3, 5, 9\}$, $A_i(s)$ is a quadrilateral with translation vector $2a_s\omega$ where ω is a unit vector in the direction of cubic root of unity. The vertices and translation vector $V_i(s)$ of $A_i(s)$ are given as follows for $i = 3, 5$ or 9 :

$$A_3(s) : \quad v_0 = \left(\frac{7}{2}s - 3, -\frac{\sqrt{3}}{2}s\right), \quad v_1 = v_0 - (2a_s, 0), \quad v_0 + b_s(-1, \sqrt{3})$$

$$v_1 + (b_s - a_s)(-1, \sqrt{3}), \quad V_3(s) = a_s(-1, \sqrt{3}).$$

The set $A_5(s)$ is a parallelogram determined by the vectors

$$v_0 + (2b_s, 0), \quad v_0 + a_s(-1, -\sqrt{3}) \quad \text{where } v_0 = \left(\frac{1}{2}s - 1, \frac{\sqrt{3}}{2}s\right).$$

The translation vector $V_5(s) = a_s(1, 0)$. The vertices of $A_9(s)$ are given as follows:

$$v_0 = \left(\frac{5}{2}s - 1, \frac{\sqrt{3}}{2}s\right), \quad v_0 + b_s(-1, \sqrt{3}), \quad v_0 + a_s(1, -\sqrt{3}s),$$

$$v_1 = (b_s - a_s)(-1, -\sqrt{3}), \quad V_9(s) = a_s(-1, -\sqrt{3}).$$

Consider the rhombus $Z_i(s) \subset A_i(s)$ of side length $2a_s$ for $i = 3, 5, 10$ as shown below in blue in Figure 17. Note that $A_i(s) \setminus Z_i(s)$ and $A_i(t)$ are same up to a scaling factor s . Denote the translation image $Z_i(s) + V_i(s)$ by $Z'_i(s)$. Note that the sets $Z'_i(s)$ and $Z_i(s)$ are adjacent in $A_i(s)$.

Let e_i be the adjacent edge between the rhombi Z_i and $Z'_i(s)$. Collapse the rhombus Z'_i towards e_i (Figure 18), and we obtain a new set \bar{X}'_s such that X_t and \bar{X}'_s are same up to a scaling by $1/s$. Moreover, there is an induced partition $\mathcal{A}'_s = \{A'_i\}_{i=0}^{10}$ of \bar{X}'_s (Figure 18) i.e.

$$A'_i(s) = \begin{cases} A_i(s) & \text{if } i = 8 \\ A_i(s) - (2a_s, 0) & \text{if } i = 2, 4 \\ A_i(s) + a_s(1, \sqrt{3}) - (2a_s, 0) & \text{if } i = 1, 10 \\ A_i(s) \setminus Z'_i(s) - V_i & \text{if } i = 3, 5, 9. \end{cases}$$

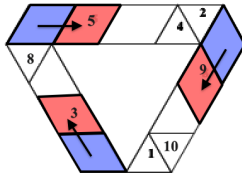


FIGURE 17. the set $Z_i(s)$ (blue) and its image $f_s(Z_i(s))$ (red) in \bar{X}_s

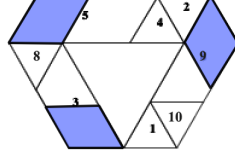


FIGURE 18. The set \bar{X}'_s for $s = 17/21$ is similar to X_t for $t = 13/17$.

We extend the map ξ_s to the set \bar{X}'_s . Thus, we have

$$\bar{X}'_t = \xi_s(\bar{X}'_s) \quad \text{and} \quad A_i(t) = \xi_s(A'_i(s)).$$

It follows that the return time for the points in $p \in Y_s$ will be equal to or longer than the return time of the point $\xi(p) \in Y_t$. Since the vectors $V_i(s)$ and $sV_i(t)$ are same up to some translations by the vectors in Λ_s or Λ_t , the images $f_s|_{Y_s}(p)$ and $f_t|_{Y_t}(\xi(p))$ must be in the corresponding positions. Hence, we have shown the first return maps $f_s|_{Y_s}$ and $f_t|_{Y_t}$ conjugates by the map ξ . \square

4.5. Induction II. Suppose $s \in (0, \frac{1}{2})$. Let $T : (0, 1) \rightarrow (0, 1)$ be the map given by

$$T(s) = \frac{s}{1+s} \quad \text{and} \quad T^{-1}(s) = \frac{s}{1-s}.$$

The map T has the action

$$[\frac{1}{2}, 1) \mapsto [\frac{1}{3}, \frac{1}{2}) \mapsto \cdots \mapsto [\frac{1}{n+1}, \frac{1}{n}) \mapsto [\frac{1}{n+2}, \frac{1}{n+1}) \mapsto \cdots.$$

Therefore,

$$(0, 1) = \bigcup_{n \geq 0} T^n([\frac{1}{2}, 1)).$$

Suppose $s \in (0, \frac{1}{2})$. Let $a_1 \geq 2$ be the first non-zero digit of the continued fraction expansion of s , then we have the relation

$$R(s) = T^{1-a_1}(s).$$

Define \diamond_k^0 (Figure 17) to be the rhombus of side length $2s$ centered at

$$((1-2k)s+1, 0) \quad \text{for} \quad k = 1, \dots, a_1-1.$$

The sides of \diamond_k are parallel to the vectors $(2, 0)$ and $(s, \sqrt{3}s)$. Define

$$Y'_s = X_s \setminus \bigcup_{k=1}^{a_1-1} \diamond_k^0.$$

Then, we obtain the subset Y_s in the Renormalization Theorem by applying the cut-and-paste operation \mathcal{OP} (Section 2.2) on the parallelogram X_s .

Similarly, we define \diamond_k^1 as the rhombus of side length $2s$ centered at

$$(2ks-1, 0) \quad \text{for} \quad k = 1, \dots, a_1-1.$$

The sides of \diamond_k^1 are parallel to the vectors $(2, 0)$ and $(-s, \sqrt{3}s)$. We call the rhombus \diamond_k^0 or \diamond_k^1 the *central tile*. Let \diamond_s be the union of all central tiles in X_s , i.e.

$$\diamond_s = \bigcup_{k=1}^{a_1-1} (\diamond_k^0 \cup \diamond_k^1).$$

The union \diamond_s remains the same under the triple lattice PET f'_s . Define \bar{Y}'_s to be the complement

$$\bar{Y}'_s = X_s \setminus \diamond_s.$$

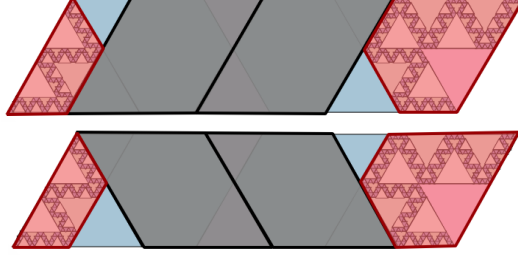


FIGURE 19. \diamond_k^0 (shaded) on the left, \diamond_k^1 (shaded) on the right for $k = 1, 2$ and \bar{Y}'_s (red)

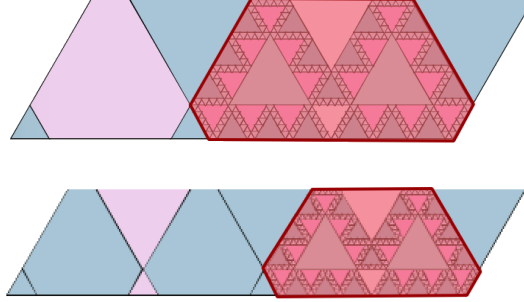


FIGURE 20. The set \bar{Y}'_t (red) for $t = 21/58$ is shown on the left and \bar{Y}'_s (red) for $s = 21/79$ is on the right. Here we provide a pictorial illustration of Induction II.

Lemma 4.3 (Induction II). *If Theorem 1.7 is true for some $u \in [\frac{1}{n}, \frac{1}{n-1}]$ for $n \geq 2$, then it holds true for $s = T(u) \in [\frac{1}{n+1}, \frac{1}{n}]$.*

Proof. We prove the statement by studying the triple lattice map f'_s and the map g_s such that $f'_s = g_s^3$. By assumption, the renormalization is true for $u \in (\frac{1}{n}, \frac{1}{n-1})$. Since

$$R(u) = R(s) \quad \text{for } s = T(u),$$

and every point is fixed under the first return map $f'_s|_{\bar{Y}'_s}$, we want to show that the restricting maps f'_s on \bar{Y}'_s and f'_u on \bar{Y}'_u is conjugate via similarities. Then, by applying the cut-and-paste operation, we obtain the desired statement.

Let P_0 and P_1 be polygons in \mathbb{R}^2 . Let Q_i be a subset of P_i such that $P_i \setminus Q_i$ has $k \geq 1$ connected components U_j^i for $i = 0, 1$ and $j = 0, \dots, k$. We say two points $p \in P_0 \setminus Q_0$ and $q \in P_1 \setminus Q_1$ are *partners* if they are in the corresponding positions relative to Q_0 and Q_1 , i.e. there exists a piecewise similarity $\alpha : P_0 \rightarrow P_1$ such that

$U_j^0 \mapsto U_j^1$ for each j , and $q = \alpha(p)$. We show that the image of a pair of partners (p_s, p_u) relative to \diamond_s and \diamond_u are also partners.

Let W_s^0 and W_s^1 be the left and right subsets of \bar{Y}'_s relative to the central tiles. If $p_s \in \bar{Y}'_s$ and $p_u \in \bar{Y}'_u$ are partners relative to \diamond_s and \diamond_u , then the associated piecewise similarity $\alpha : X_s \rightarrow X_u$ is given by

$$\alpha_s(p_s) = \begin{cases} \frac{1}{1-s}(p_s - V_s^0) + V_u^0 & \text{if } p_s \in W_s^0 \\ \frac{1}{1-s}(p_s - V_s^1) + V_u^1 & \text{if } p_s \in W_s^1 \end{cases}$$

where V_ω^0 and V_ω^1 are the lower left and right vertices of X_ω respectively for $\omega \in \{s, u\}$.

Let the points $p_s \in X_s \setminus \diamond_s$ and $p_u \in X_u \setminus \diamond_u$ be partners. Let v_s and v_t be the vectors in $(L_0)_s$ and $(L_0)_u$ (Section 1.3) such that $p_s + v_s \in (F_1)_s$ and $p_u + v_u \in (F_1)_u$. Depending on the position of right and left respect to the diamonds, the vector $\nu = v_s - (1-s)v_u$ belongs to one of the following three case:

- 1) $\nu = (-s, \sqrt{3}s)$ if p_s and p_u belong to left triangle in Y'_s and Y'_u respectively.
- 2) $\nu = (-2s, 0)$ if p_s and p_u belongs to the parallelogram right to the central tiles.
- 3) $\nu = (-2s, 0) + (-s, \sqrt{3}s)$ otherwise.

It follows that the image $g_s(p_s)$ and $g_u(p_u)$ are in the corresponding positions relative to $g_s(\diamond_s)$ and $g_u(\diamond_u)$.

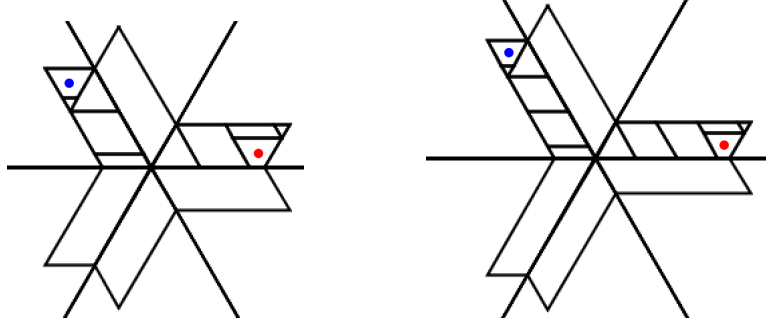


FIGURE 21. Partners (p_s, p_u) (red) and $(g_s(p_s), g_u(p_u))$ for $u = 7/17$ and $s = T(u) = 7/24$

Similarly, a pair of partners $(p_s \in (F_1)_s, p_u \in (F_1)_u)$ relative to $g(\diamond_s)$ and $g(\diamond_u)$ becomes partners relative to $g_s^2(\diamond_s)$ and $g_u^2(\diamond_u)$ under the maps g_s and g_u . Let $\nu = v_s = (1-s)v_u$ where v_s and v_u are defined similarly as before. The vector $\nu = v_s - (1-s)v_u$ is

$$(s, -\sqrt{3}s), \quad -(s, \sqrt{3}s) \quad \text{and} \quad (0, -2\sqrt{3}s) = -(s, \sqrt{3}s) + (s, -\sqrt{3}s)$$

depending on whether or not p_s, p_u and their image lie in the top or bottom of the F_1 and F_2 respectively. Same argument works for pair of partners in $(F_2)_s$ and $(F_s)_u$ for the vector $\nu = v_s - (1-s)v_u$ is one of the following forms depending on the positions of the points p_s, p_u and their image in the parallelograms

$$(2s, 0), \quad (s, \sqrt{3}s), \quad \text{and} \quad (3s, \sqrt{3}s) = (2s, 0) + (s, \sqrt{3}s).$$

It follows that the maps f_s and f_u restricting on the sets \bar{Y}_s and \bar{Y}_u are conjugate via a map of similarity. Therefore, we have shown the inductive step for the renormalization on the interval $(0, \frac{1}{2})$. \square

5. SYMMETRY

In this section, we analyze the symmetries of the periodic pattern Δ_s for $s \in [8/13, 13/21]$, which will help us to understand the properties of the limit set Λ_ϕ later.

5.1. Symmetry 1. Let $s \in [8/13, 13/21]$ and A, B and C be isosceles trapezoids in X_s as illustrated in Figure 22. In this section, we will show that the periodic tiles in A, B and C are same up to rotation and reflection.

Here we give a precise description of the trapezoids A, B and C . The vertices of trapezoid A are

$$v_0 = \left(-1 + \frac{1}{2}s, \frac{\sqrt{3}}{2}s\right), \quad v_1 = v_0 + s(1, -\sqrt{3})$$

$$v_2 = v_0 - (1-s)(1, \sqrt{3}), \quad \text{and} \quad v_3 = v_1 - 2(1-s)(1, 0).$$

The quadrilateral A is an isosceles trapezoid of base angle $\pi/3$ and side length $2(2s-1)$, $2(1-s)$ and $2s$. For the trapezoid B and C , let μ_s be the map of rotation by $\pi/3$ about the upper left vertex of the parallelogram X_s , and ν_s be the map of reflection about the vertical line $x = \frac{3}{2}s - 1$. The trapezoids B and C are obtained by the formulas

$$B = \mu_s(A) \quad \text{and} \quad C = \nu_s(A).$$

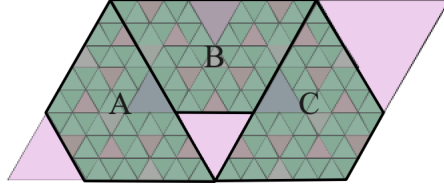


FIGURE 22. L_s (lightly shaded triangle) and M_s (transparent triangle) for $s = 8/13$

The following lemma shows that there exists rotational symmetry between periodic pattern restricting in A and B , and a reflectional symmetry between the periodic patterns in subsets A and C .

Lemma 5.1. *Suppose $s \in [8/13, 13/21]$. Then, the following two equations are satisfied on M_s and N_s respectively:*

$$(1) \quad \mu_s \circ f_s|_A \circ \mu_s^{-1} = f_s^{-1}|_B.$$

$$(2) \quad \nu_s \circ f_s|_A \circ \nu_s^{-1} = f_s^{-1}|_C.$$

The proof follows the similar scheme as the one for the base case of the Renormalization theorem (Section 4.2). Here we explain the differences.

Recall that \mathcal{X} is the fiber bundle over $[1/2, 1]$. We define $\mathbf{A} \subset \mathcal{X}$ to be the polyhedron over the interval $[8/13, 13/21]$ such that the fiber above s is the isosceles trapezoid A_s , i.e.

$$\mathbf{A} = \{(x, y, s) | (x, y) \in A_s \text{ and } s \in [8/13, 13/21]\}.$$

Let $F : \mathcal{X} \rightarrow \mathcal{X}$ be the fiber bundle map on \mathcal{X} . Let \mathcal{S} be a subset of \mathcal{X} . A *maximal return domain* in \mathcal{S} under the map F is a maximal subset of the return map $F|_{\mathcal{S}}$ where $F|_{\mathcal{S}}$ is entirely defined and continuous.

With computer assistance, we find that there are 12 maximal return domains α_i in \mathbf{A} , each of which is a convex polytope, i.e.

$$\mathbf{A} = \alpha_0 \cup \alpha_1 \cdots \cup \alpha_{10}.$$

Moreover, the vertices of each maximal domain α_i are of the format

$$\begin{bmatrix} (m_0 s_0 + n_0)/2 \\ (p_0 s_0 + q_0)\sqrt{3}/2 \\ s_0 \end{bmatrix} \begin{bmatrix} (m_0 s_1 + n_0)/2 \\ (p_0 s_1 + q_0)\sqrt{3}/2 \\ s_1 \end{bmatrix} \cdots \begin{bmatrix} (m_{k-1} s_0 + n_{k-1})/2 \\ (p_{k-1} s_0 + q_{k-1})\sqrt{3}/2 \\ s_0 \end{bmatrix} \begin{bmatrix} (m_{k-1} s_1 + n_{k-1})/2 \\ (p_{k-1} s_1 + q_{k-1})\sqrt{3}/2 \\ s_1 \end{bmatrix}.$$

where $m_j, n_j, p_j, q_j \in \mathbb{Z}$ for $0 < j < k$, $s_0 = 8/13$ and $s_1 = 13/21$. Same as the fiber bundle map $F : \mathcal{X} \rightarrow \mathcal{X}$, the first return map $F|_{\mathbf{A}}$ is an piecewise affine map on each maximal return domain α_i partitioning \mathbf{A} . Let α be a maximal return domain in \mathbf{A} , for $(x, y, z) \in \alpha$, the map $F|_{\mathbf{A}}$ has action

$$(x, y, z) \mapsto (x, y, z) + \left(\frac{az + b}{2}, \frac{cz + d}{2}\sqrt{3}, 0 \right), \quad a, b, c, d \in \mathbb{Z}.$$

We call (a, b, c, d) the *coefficient tuple* of the maximal return domain. For convenience, we write maximal return domains of the map $F|_{\mathbf{A}}$ along with their coefficient tuples in matrix format:

$$\begin{bmatrix} m_0 & n_0 & p_0 & q_0 \\ m_1 & n_1 & p_1 & q_1 \\ \vdots & \vdots & \vdots & \vdots \\ m_{k-1} & n_{k-1} & p_{k-1} & q_{k-1} \\ a & b & c & d \end{bmatrix}.$$

The list of all maximal return domains partitioning polytope \mathbf{A} is provided in Section 7.2.

Define the affine map $\Upsilon : \mathcal{X} \rightarrow \mathcal{X}$ by piecing together all the rotations μ_s for $s \in [8/13, 13/21]$, i.e.

$$\Upsilon(x, y, s) = (\mu_s(x, y), s)$$

The rest of the calculation is the same as the one in Section 4.2.

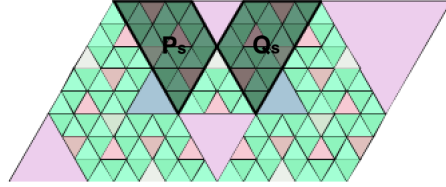


FIGURE 23. An illustration of reflectional symmetry of periodic patterns

5.2. Symmetry 2. Let P_s be a isosceles trapezoid of the symmetric piece M_s with base angle $\pi/3$ such that P_s has vertices

$$\begin{bmatrix} \frac{1}{2}s - 1 \\ \frac{\sqrt{3}}{2}s \end{bmatrix} \begin{bmatrix} \frac{9}{2}s - 3 \\ \frac{\sqrt{3}}{2}s \end{bmatrix} \begin{bmatrix} \frac{3}{2}s - 1 \\ (\frac{7}{2}s - 2)\sqrt{3} \end{bmatrix} \begin{bmatrix} -\frac{s}{2} \\ (\frac{3}{2}s - 1)\sqrt{3} \end{bmatrix}.$$

Let $\iota_s : X_s \rightarrow X_s$ be the reflection about the vertical line $x = \frac{3}{2}s - 1$. Define the set Q_s as

$$Q_s = \iota(P_s).$$

The following lemma states that the periodic tiles in P_s and the ones in Q_s are same up to reflection ι_s .

Lemma 5.2. *Suppose $s \in [8/13, 13/21]$, then*

$$\iota_s \circ f_s^{-1}|_{P_s} \circ \iota_s = f_s|_{Q_s}.$$

We apply the same method as the proof of Lemma 4.1. Define \mathcal{Q} be the fiber bundle over $[8/13, 13/21]$

$$\mathcal{Q} = \{(x, y, s) | (x, y) \in Q_s \text{ and } s \in [8/13, 13/21]\}.$$

The list of maximal return domains in the polyhedra \mathcal{Q} along with their coefficient tuples are provided in Section 7.

6. LIMIT SET Λ_ϕ FOR $\phi = \frac{\sqrt{5}-1}{2}$

In this section, we describe one application of our main theorem. We show that Δ_ϕ is dense. We explore the properties of the limit set Λ_ϕ where ϕ is the only fixed point under the renormalization map R . Denote symmetric trapezoids defined in Section 5.1 as A, B and C for $s = \phi$. We call the trapezoids A, B and C the *fundamental trapezoids*.

6.1. Shield Lemma. Let l_0 be the line such that the intersection $A \cap B$ belongs to l_0 . We say that a polygon P *abuts* on l_0 if P has an edge contained in l_0 . We call such segment a *contact*.

Lemma 6.1 (Shield). *Let V be the top left vertex of X_s . There is a sequence of periodic tiles $\{P_n\}_{n=0}^\infty$ satisfying the following properties:*

- (1) *Each element P_n is an equilateral triangle abutting the line segment l_0 .*
- (2) *The sequence occur in a monotone decreasing size. The periodic tile P_{n+1} is similar to P_n of scaling factor ϕ for all $n \geq 0$.*
- (3) *The periodic tiles in the sequence, from largest to smallest, move towards the point V .*
- (4) *For any point $p \in l_0 \setminus V$, there must be a periodic tile P_n in the sequence whose contact of positive length contains p .*

Proof. Let P_0 be a fixed periodic tile of X_ϕ under the map f_s (Figure 24). The tile P_0 is an equilateral triangle of side length $4s - 2$ with a horizontal top side. The bottom vertex has coordinate $(3s/2 - 1, -\sqrt{3}/2)$. The triangle P_0 abuts the line l_0 . Recall the map of similarity ψ_s in Theorem 1.7 taking the subset Y_s to $X_{R(s)}$. For convenience, we write ζ as the inverse ψ_ϕ^{-1} . The scaling factor of the similarity ζ is $\phi = \frac{-1+\sqrt{5}}{2}$.

Consider a sequence $\{P_n\}_{n=0}^\infty$ such that

$$P_n = \zeta^n(P_0).$$

Since ϕ is fixed by the renormalization map R , each P_n is a periodic equilateral triangle of X_ϕ . Note that the line l_0 is invariant under the map ζ so that each periodic P_n abuts to l_0 . Moreover, the triangles P_n in the sequence point towards different

side of l_0 alternatively. Therefore, we have shown statement 1, and statement 2 and 3 follow directly.

According to the renormalization and properties of the map ξ

$$P_i \cap P_j = \begin{cases} \emptyset & \text{if } j \neq i \pm 1 \\ v & \text{otherwise} \end{cases}$$

where v is vertex for both P_i and P_j . Therefore, for any point $p \in l_0 \setminus V$, there must exist an element $P_n = \zeta^n(P_0)$ for some $n \geq 0$ such that P_n has a side of positive length on l_0 containing p . \square

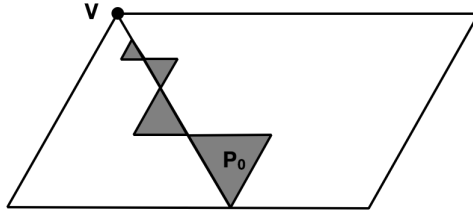


FIGURE 24. The sequence of periodic tiles in Lemma 5.1

Corollary 6.2. *Every point $p \in l_0 \setminus V$ is contained in the edge of a periodic triangle given by the map f_ϕ .*

Note that the union of the fundamental trapezoids $A \cup B \cup C$ contains all periodic tiles $\Delta_p \in \Delta$, except for three fixed periodic triangles, so

$$\Lambda_\phi \subset A \cup B \cup C.$$

Let $S \subset X_s$ be a subset and $\Lambda_\phi(S) = \Lambda_\phi \cap S$. The Shield lemma implies that

$$\Lambda_\phi(A) \cap \Lambda_\phi(B) = \{\xi^{-n}(V_0)\}_{n=1}^\infty$$

where V_0 is the bottom vertex of P_0 .

6.2. Substitution Rule. In this section, we provide a precise description of the substitution rule introduced in Section 1.7. Let M be an isosceles trapezoid such that the base angles of M are $\pi/3$. The parallel sides of M are of side length $2s$ and $2(1 - s)$, and two non-parallel ones are of length $2(2s - 1)$. The trapezoid M is substituted by three similar isosceles trapezoids M_1, M_2 and M_3 of scaling factor ϕ, ϕ^2 and ϕ respectively (Figure 25). The non-parallel sides of M become the longest parallel sides of M_1 and M_3 , and the top side of M becomes the longer parallel side of M_2 . Note that the trapezoids M_1 and M_3 are same up to reflection about the vertical line passing through the midpoint of the parallel sides of M .

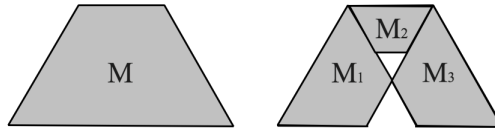


FIGURE 25. Substitution rule

We apply the substitution on each fundamental trapezoid. By symmetries, we can restrict our focus to the substitution of the isosceles trapezoid A . Let A_1 , A_2 and A_3 be the three substituted trapezoids of A as shown in Figure 26. We have the following observations:

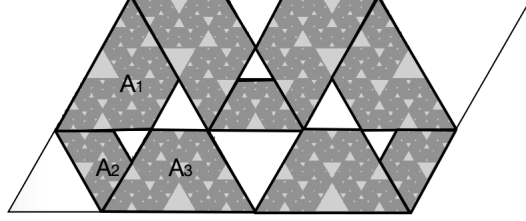


FIGURE 26. The substitution on fundamental trapezoids A , B and C

- (1) Denote the equilateral triangle bounded by sides of A , B and C by P_0 . The triangle P_0 is a fixed periodic tile under the map f_ϕ . Recall the map $\xi = \psi_\phi^{-1}$ where ψ_ϕ is the map of similarity for renormalization. Let ι_1 be the reflection about the line $l_1 : y = \frac{\sqrt{3}}{3}(x + 1 - s)$ where $l_1 = \xi(l)$ and $l : x = \frac{3}{2}s - 1$ is the line of reflectional symmetry. The set $A \setminus \bigcup_{i=1}^3 A_i$ is composed of two triangles:

$$\xi(P_0) \quad \text{and} \quad \iota_1 \circ \xi^2(P_0).$$

Since the triangle P_0 is a periodic tile of f_ϕ , according to renormalization and symmetry of f_s , both triangles $\xi(P_0)$ and $\iota_1 \circ \xi^2(P_0)$ are periodic tiles in containing in the fundamental trapezoid A .

- (2) Let $S \subset X_s$ and $\Delta(S) = \Delta_\phi \cap S$ be the restriction of the periodic pattern Δ_ϕ on S . Then $\Delta(A_i)$ is same as $\Delta(A)$ up to a map of similarity for all $i \in \{1, 2, 3\}$. To see this, recall that μ_s is the map of rotation about the top left vertex of X_s by $\pi/3$. We have the relations

$$A_1 = \mu_\phi \circ \xi(A), \quad A_2 = \mu_\phi \circ \xi^2(A) \quad \text{and} \quad A_3 = \iota_1(A_1).$$

Lemma 6.3. *The periodic pattern Δ_ϕ is dense.*

Proof. By symmetries, we restrict our focus to the fundamental trapezoid A . We show that any point $p \in A$ is within ϵ of some periodic tiles. According to previous discussion, the fundamental trapezoid A is partitioned into a finite union of periodic tiles and a finite union of trapezoids which are same as A up to similarities. The similarities are contractions by the factor ϕ^n for $n \geq 0$. We call a trapezoid which is similar to A and obtained by substitutions an ϵ -patch if its longest side has length $l_e \leq \epsilon$.

By iterating the substitution, for any $p \in A$, we have $p \in \Delta_p$ for some periodic tile Δ_p or p must lie in some ϵ -patch K . For the first case, we are done. If $p \in K$ for some ϵ -patch K , then K must contain a periodic triangle by previous discussion. Therefore, the point p lie within ϵ of the periodic tile. \square

6.3. Proof of Theorem 1.7. In this section, we show that the limit set Λ_ϕ can be obtained by a sequence of substitutions on the fundamental trapezoids.

Let $\mathcal{C}_0 = A \cup B \cup C$. The set \mathcal{C}_{n+1} is defined inductively as the union of all trapezoids given by applying substitution rule on each trapezoid in \mathcal{C}_n for $n \geq 0$. We call the trapezoids in \mathcal{C}_n marked trapezoids. Define

$$L\Lambda = \lim_{n \rightarrow \infty} \mathcal{C}_n.$$

Here we show that

$$L\Lambda = \Lambda_\phi.$$

“ \subseteq ” Take an arbitrary point $p \in L\Lambda$. Since the sequence of chains $\{\mathcal{C}_n\}_0^\infty$ is a nested family of unions of marked trapezoids, any neighborhood of p intersects an infinite sequence of marked trapezoids. According to previous section, each marked trapezoid contains infinitely many periodic tiles. Therefore, we have $p \in \Lambda_\phi$.

“ \supseteq ” Take a point $p \in \Lambda_\phi$, then every neighborhoods U_p of p intersects infinitely many periodic tiles. There must exists a trapezoids $M \in \mathcal{C}_{n_0}$ so that $p \in M$ and $M \cap U_p \neq \emptyset$. Otherwise, p must be in some periodic tile, which leads to a contradiction. We want to show that p belongs to the chain \mathcal{C}_n for every $n \geq n_0$. Suppose there exists a marked trapezoid M_n such that $p \in M_n \setminus M'$ for any marked trapezoid $M' \subset M$ and $M' \in \mathcal{C}_{n+1}$, then there is a neighborhood of p intersecting only finitely many periodic tiles in Δ_ϕ . Contradiction. \square

6.4. Proof of Theorem 1.9. Because of the reflection and rotational symmetries of the fundamental trapezoids A, B and C , we restrict our focus on the substitutions in trapezoid A in the chain \mathcal{C}_0 first. Let σ_i be the similarity on the trapezoid A to smaller trapezoids A_i by substitution for $i = 1, 2$ and 3 . Let $\Lambda_\phi|_A$ be the limit set Λ_ϕ restricting on A . By construction, the limit set $\Lambda_\phi|_A$ is the attractor of the iterated function system given by the similarites $\{\sigma_i\}_{i=1}^3$, i.e.

$$\Lambda_\phi|_A = \bigcup_{i=1}^3 \sigma_i(\Lambda_\phi|_A).$$

To compute the Hausdorff dimension of Λ_ϕ , we check the open set condition (Section 2.5). The condition holds simply by taking the open set V as the interior of A . Thus, according to Theorem 9.3 in [5], we have the equation:

$$2\phi^s + \phi^{2s} = 1.$$

The Hausdorff dimension for Λ_ϕ in the polygon A is

$$s = \frac{\log(-1 + \sqrt{2})}{\log \phi} = 1.83147\dots$$

Same computation on the limit set Λ_ϕ restricting in the trapezoids B and C . By elementary properties of Hausdorff dimension, we have

$$1 < \dim_H(\Lambda_\phi) = \frac{\log(-1 + \sqrt{2})}{\log \phi} = 1.83147\dots < 2. \quad \square$$

7. THE COMPUTATIONAL DATA

7.1. Data of Maximal Domains. Here we list all the maximal domains D_i of the fiber bundle \mathcal{X} for the map F and their coefficient tuples ω_i for $i = 0, \dots, 11$. To have a nicer form, we scale the y -coordinates by $1/\sqrt{3}$.

$$\begin{aligned}
D_0 &: \begin{bmatrix} 2/3 \\ 1/2 \\ 1 \end{bmatrix} \begin{bmatrix} 5/4 \\ 1/4 \\ 1/2 \end{bmatrix} \begin{bmatrix} 1/4 \\ 1/4 \\ 1/2 \end{bmatrix} \begin{bmatrix} 3/4 \\ -1/4 \\ 1/2 \end{bmatrix}, \quad \omega_0 = [0, 0, 0, 0]; & D_1 &: \begin{bmatrix} 1/2 \\ -1/2 \\ 1 \end{bmatrix} \begin{bmatrix} 1/4 \\ 1/4 \\ 1/2 \end{bmatrix} \begin{bmatrix} 3/4 \\ -1/4 \\ 1/2 \end{bmatrix} \begin{bmatrix} -1/4 \\ -1/4 \\ 1/2 \end{bmatrix} \begin{bmatrix} 1/4 \\ -1/4 \\ 1/2 \end{bmatrix}, \quad \omega_1 = [2, -2, 0, 0]; \\
D_2 &: \begin{bmatrix} 3/4 \\ 1/4 \\ 1 \end{bmatrix} \begin{bmatrix} 0 \\ 1/6 \\ 2/3 \end{bmatrix} \begin{bmatrix} 1/8 \\ 1/8 \\ 1/2 \end{bmatrix} \begin{bmatrix} -1/8 \\ -1/8 \\ 1/2 \end{bmatrix}, \quad \omega_2 = [0, -1, -2, 1]; & D_3 &: \begin{bmatrix} -1/2 \\ 1/2 \\ 1 \end{bmatrix} \begin{bmatrix} 1/2 \\ -1/2 \\ 1 \end{bmatrix} \begin{bmatrix} -2/3 \\ -1/3 \\ 2/3 \end{bmatrix} \begin{bmatrix} -1/4 \\ -1/4 \\ 1/2 \end{bmatrix}, \quad \omega_3 = [1, -1, -1, 1]; \\
D_4 &: \begin{bmatrix} 3/2 \\ 1/2 \\ 1 \end{bmatrix} \begin{bmatrix} -3/4 \\ 1/4 \\ 1/2 \end{bmatrix} \begin{bmatrix} -1/4 \\ -1/4 \\ 1/2 \end{bmatrix} \begin{bmatrix} -5/4 \\ -1/4 \\ 1/2 \end{bmatrix}, \quad \omega_4 = [-2, 2, 0, 0]; & D_5 &: \begin{bmatrix} 3/2 \\ 1/2 \\ 1 \end{bmatrix} \begin{bmatrix} -1/2 \\ 1/2 \\ 1 \end{bmatrix} \begin{bmatrix} -3/4 \\ 1/4 \\ 1/2 \end{bmatrix} \begin{bmatrix} -5/4 \\ -1/4 \\ 1/2 \end{bmatrix}, \quad \omega_5 = [-2, 2, 0, 0]; \\
D_6 &: \begin{bmatrix} -1/2 \\ 1/2 \\ 1 \end{bmatrix} \begin{bmatrix} 1/2 \\ -1/2 \\ 1 \end{bmatrix} \begin{bmatrix} -3/2 \\ -1/2 \\ 1 \end{bmatrix} \begin{bmatrix} -5/4 \\ -1/4 \\ 1/2 \end{bmatrix}, \quad \omega_6 = [0, 0, 0, 0]; & D_7 &: \begin{bmatrix} 0 \\ 1/3 \\ 2/3 \end{bmatrix} \begin{bmatrix} 1/4 \\ 1/4 \\ 1/2 \end{bmatrix} \begin{bmatrix} -3/4 \\ 1/4 \\ 1/2 \end{bmatrix} \begin{bmatrix} -1/4 \\ -1/4 \\ 1/2 \end{bmatrix}, \quad \omega_7 = [0, 0, 0, 0]; \\
D_8 &: \begin{bmatrix} -1/2 \\ 1/4 \\ 1 \end{bmatrix} \begin{bmatrix} -2/3 \\ -1/3 \\ 2/3 \end{bmatrix} \begin{bmatrix} -1/4 \\ -1/4 \\ 1/2 \end{bmatrix} \begin{bmatrix} -5/4 \\ -1/4 \\ 1/2 \end{bmatrix}, \quad \omega_8 = [2, 0, 0, 0]; & D_9 &: \begin{bmatrix} 2/3 \\ 1/2 \\ 1 \end{bmatrix} \begin{bmatrix} 1/2 \\ -1/2 \\ 1 \end{bmatrix} \begin{bmatrix} 1 \\ 0 \\ 2/3 \end{bmatrix} \begin{bmatrix} 1/4 \\ 1/4 \\ 1/2 \end{bmatrix}, \quad \omega_9 = [1, -1, 1, -1]; \\
D_{10} &: \begin{bmatrix} 1/2 \\ -1/2 \\ 1 \end{bmatrix} \begin{bmatrix} 1 \\ 0 \\ 2/3 \end{bmatrix} \begin{bmatrix} 1/4 \\ 1/4 \\ 1/2 \end{bmatrix} \begin{bmatrix} 3/4 \\ -1/4 \\ 1/2 \end{bmatrix}, \quad \omega_{10} = [0, -1, 2, -1]; & D_{11} &: \begin{bmatrix} 3/2 \\ 1/2 \\ 1 \end{bmatrix} \begin{bmatrix} -1/2 \\ 1/2 \\ 1 \end{bmatrix} \begin{bmatrix} 1/2 \\ -1/2 \\ 1 \end{bmatrix} \begin{bmatrix} -1/4 \\ -1/4 \\ 1/2 \end{bmatrix}, \quad \omega_{11} = [0, 0, 0, 0].
\end{aligned}$$

7.2. Maximal Return Domains for Symmetry 1. Here is the list of all the maximal return domains in \mathbf{A} along with their coefficient tuple of matrix format:

$$\begin{aligned}
\alpha_0 &: \begin{bmatrix} -5 & 1 & -1 & 0 \\ 3 & -2 & -1 & 0 \\ -1 & 0 & 3 & -2 \\ 2 & -2 & -2 & 2 \end{bmatrix}, & \alpha_1 &: \begin{bmatrix} 7 & -6 & -1 & 0 \\ -5 & 2 & -1 & 0 \\ -3 & 0 & 9 & -6 \\ -9 & 4 & 3 & -2 \\ 8 & -4 & 0 & 0 \end{bmatrix}, & \alpha_2 &: \begin{bmatrix} -5 & 2 & -1 & 0 \\ 1 & -2 & -7 & 4 \\ -11 & 6 & -7 & 4 \\ -4 & 2 & 4 & -2 \end{bmatrix} \\
\alpha_3 &: \begin{bmatrix} -3 & 0 & 9 & -6 \\ 3 & -4 & 3 & -2 \\ -9 & 4 & 3 & -2 \\ 8 & -4 & 0 & 0 \end{bmatrix}, & \alpha_4 &: \begin{bmatrix} 1 & -2 & -7 & 4 \\ -11 & 6 & -7 & 4 \\ 11 & -4 & 3 & -2 \\ -1 & 0 & 3 & -2 \\ 6 & -4 & 6 & -4 \end{bmatrix}, & \alpha_5 &: \begin{bmatrix} 1 & -2 & -7 & 4 \\ -9 & 4 & 3 & -2 \\ 11 & -4 & 3 & -2 \\ 0 & 0 & 0 & 0 \end{bmatrix} \\
\alpha_6 &: \begin{bmatrix} 23 & -8 & 3 & -2 \\ 11 & -8 & 3 & -2 \\ 17 & -12 & -3 & 2 \\ -6 & 4 & 6 & -4 \end{bmatrix}, & \alpha_7 &: \begin{bmatrix} 11 & -8 & 3 & -2 \\ -1 & 0 & 3 & -2 \\ 5 & -2 & -3 & 2 \\ 0 & 0 & 0 & 0 \end{bmatrix}, & \alpha_8 &: \begin{bmatrix} 3 & -4 & 3 & -2 \\ 23 & -16 & 3 & -2 \\ -3 & 0 & -3 & 2 \\ 17 & -12 & -3 & 2 \\ -12 & 8 & 0 & 0 \end{bmatrix} \\
\alpha_9 &: \begin{bmatrix} 11 & -8 & 3 & -2 \\ 5 & -2 & -3 & 2 \\ 7 & -6 & 7 & -4 \\ -5 & 2 & 7 & -4 \\ -4 & 2 & -4 & 2 \end{bmatrix}, & \alpha_{10} &: \begin{bmatrix} -3 & 0 & -3 & 2 \\ 17 & -12 & -3 & 2 \\ 7 & -6 & 7 & -4 \\ -2 & 2 & 2 & -2 \end{bmatrix}, & \alpha_{11} &: \begin{bmatrix} 7 & -6 & 7 & -4 \\ -5 & 2 & 7 & -4 \\ 1 & -2 & 1 & 0 \\ -4 & 2 & -4 & 2 \end{bmatrix}
\end{aligned}$$

7.3. Maximal Return Domains for Symmetry 2. Here are 10 maximal return domains $\alpha_0, \dots, \alpha_9$ in \mathbf{Q} along with their coefficient tuples of matrix format:

$$\begin{aligned}
\alpha_0 &: \begin{bmatrix} 7 & -4 & 3 & -2 \\ -3 & 2 & 13 & -8 \\ 2 & 0 & -3 & 2 \\ -9 & 6 & 7 & -4 \\ 6 & -4 & -6 & 4 \end{bmatrix}, & \alpha_1 &: \begin{bmatrix} -3 & 2 & 13 & -8 \\ 13 & -8 & -3 & 2 \\ -19 & 12 & -3 & 2 \\ 4 & -2 & 4 & -2 \end{bmatrix}, & \alpha_2 &: \begin{bmatrix} 13 & -8 & -3 & 2 \\ -19 & 12 & -3 & 2 \\ 3 & -2 & 7 & -4 \\ -29 & 18 & 7 & -4 \\ 20 & -12 & 0 & 0 \end{bmatrix} \\
\alpha_3 &: \begin{bmatrix} 2 & 0 & -3 & 2 \\ -9 & 6 & 7 & -4 \\ 11 & -6 & 7 & -4 \\ 0 & 0 & 0 & 0 \end{bmatrix}, & \alpha_4 &: \begin{bmatrix} -19 & 12 & -3 & 2 \\ -29 & 18 & 7 & -4 \\ -9 & 6 & 7 & -4 \\ 10 & -6 & 10 & -6 \end{bmatrix}, & \alpha_5 &: \begin{bmatrix} 23 & -14 & 7 & -4 \\ -9 & 6 & 7 & -4 \\ 7 & -4 & -9 & 6 \\ 0 & 0 & 0 & 0 \end{bmatrix} \\
\alpha_6 &: \begin{bmatrix} -9 & 6 & 7 & -4 \\ 11 & -6 & 7 & -4 \\ 27 & -16 & -9 & 6 \\ -10 & 6 & 10 & -6 \end{bmatrix}, & \alpha_7 &: \begin{bmatrix} 3 & -2 & 7 & -4 \\ 23 & -14 & 7 & -4 \\ -3 & 2 & 1 & 0 \\ 17 & -10 & 1 & 0 \\ -12 & 8 & 0 & 0 \end{bmatrix}, & \alpha_8 &: \begin{bmatrix} 7 & -4 & -9 & 6 \\ 27 & -16 & -9 & 6 \\ 17 & -10 & 1 & 0 \\ 6 & -4 & 6 & -4 \end{bmatrix} & \alpha_9 &: \begin{bmatrix} 11 & -6 & 7 & -4 \\ 17 & -10 & 1 & 0 \\ 5 & -2 & 1 & 0 \\ -4 & 2 & -4 & 2 \end{bmatrix}
\end{aligned}$$

REFERENCES

- [1] R. Adler, B. Kitchens, and C. Tresser. Dynamics of non-ergodic piecewise affine maps of the torus. *Ergodic Theory Dynam. Systems*, 21(4):959–999, 2001.
- [2] S. Akiyama and E. Harriss. Pentagonal domain exchange. *Discrete Contin. Dyn. Syst.*, 33(10):4375–4400, 2013.
- [3] N. Bedaride and J.–F. Bertazzon. An example of pet. computation of the hausdorff dimension of the aperiodic set. *To appear Transactions of the AMS*, 2016.
- [4] J. Buzzi. Piecewise isometries have zero topological entropy. *Ergodic Theory Dynam. Systems*, 21(5):1371–1377, 2001.
- [5] K. Falconer. *Fractal geometry*. John Wiley & Sons, Ltd., Chichester, third edition, 2014. Mathematical foundations and applications.
- [6] A. Goetz. Dynamics of piecewise isometries. *Illinois J. Math.*, 44(3):465–478, 2000.
- [7] A. Goetz. Piecewise isometries—an emerging area of dynamical systems. In *Fractals in Graz 2001*, Trends Math., pages 135–144. Birkhäuser, Basel, 2003.
- [8] A. Goetz and G. Poggiaspalla. Rotations by $\pi/7$. *Nonlinearity*, 17(5):1787–1802, 2004.
- [9] E. Gutkin and N. Haydn. Topological entropy of polygon exchange transformations and polygonal billiards. *Ergodic Theory Dynam. Systems*, 17(4):849–867, 1997.
- [10] H. Haller. Rectangle exchange transformations. *Monatsh. Math.*, 91(3):215–232, 1981.
- [11] P. Hooper. Renormalization of polygon exchange maps arising from corner percolation. *Invent. Math.*, 191(2):255–320, 2013.
- [12] M. Keane. Interval exchange transformations. *Math. Z.*, 141:25–31, 1975.
- [13] J. H. Lowenstein. Aperiodic orbits of piecewise rational rotations of convex polygons with recursive tiling. *Dyn. Syst.*, 22(1):25–63, 2007.
- [14] J. H. Lowenstein, K. L. Kouptsov, and F. Vivaldi. Recursive tiling and geometry of piecewise rotations by $\pi/7$. *Nonlinearity*, 17(2):371–395, 2004.
- [15] G. Rauzy. échanges d’intervalles et transformations induites. *Acta Arith.*, 34(4):315–328, 1979.
- [16] R.E. Schwartz. Outer billiards on the Penrose kite: compactification and renormalization. *J. Mod. Dyn.*, 5(3):473–581, 2011.
- [17] R.E. Schwartz. *The octagonal PETs*, volume 197 of *Mathematical Surveys and Monographs*. American Mathematical Society, Providence, RI, 2014.
- [18] M. Viana. Ergodic theory of interval exchange maps. *Rev. Mat. Complut.*, 19(1):7–100, 2006.
- [19] J-C. Yoccoz. Continued fraction algorithms for interval exchange maps: an introduction. In *Frontiers in number theory, physics, and geometry. I*, pages 401–435. Springer, Berlin, 2006.
- [20] A. Zorich. Flat surfaces. In *Frontiers in number theory, physics, and geometry. I*, pages 437–583. Springer, Berlin, 2006.

DEPARTMENT OF MATHEMATICS, BROWN UNIVERSITY, PROVIDENCE, RHODE ISLAND 02912
E-mail address: renyi@math.brown.edu